Journal of Crystal Growth 532 (2020) 125433

Contents lists available at ScienceDirect

Journal of Crystal Growth

journal homepage: www.elsevier.com/locate/jcrysgro

Unsteady numerical simulations considering effects of thermal stress and heavy doping on the behavior of intrinsic point defects in large-diameter Si crystal growing by Czochralski method

Yuji Mukaiyama[a,*], Koji Sueoka[d], Susumu Maeda[c], Masaya Iizuka[a], Vasif M. Mamedov[b]

[a] STR Japan K.K., East Tower 15F, Yokohama Business Park, 134, Goudo-cho, Hodogaya-ku, Yokohama, Kanagawa 240-0005, Japan
[b] STR Group—Soft-Impact, Ltd., Bolshoi Sampsonievskii pr. 64, Build. "E", 194044 St. Petersburg, Russia
[c] GlobalWafers Japan Co., Ltd., 6-861-5 Higashiko, Seiro, Niigata 957-0197, Japan
[d] Okayama Prefectural University, 111 Kuboki, Soja, Okayama 719-1197, Japan

ARTICLE INFO

Communicated by Chung wen Lan

Keywords:
A1. Computer simulation
A1. Point defects
A1. Stresses
A2. Czochralski method
B2. Semiconducting silicon

ABSTRACT

We conducted unsteady simulations of intrinsic point defect dynamics considering the effects of the thermal stress and dopant concentration in a large-diameter silicon crystal growing by the Czochralski (Cz) method. The thermal equilibrium concentration of the intrinsic point defects (vacancy, *V*, and self-interstitial Si atom, *I*) was simulated as a function of the thermal stress and the incorporated dopant concentration in a growing Si crystal, which was obtained through *ab-initio* calculations. Furthermore, point defect dynamics in the crystal were solved within a two-dimensional axisymmetric unsteady global heat and mass transport model by considering the thermal stress and the incorporation of a dopant using segregation for dynamically pulling Si crystal by the Cz method. The unsteady numerical simulations showed that the formation and the distribution of intrinsic point defects depend on the temporal variation of the thermal stress and the incorporated dopant concentration in a growing Si crystal.

1. Introduction

Recently, continuous quality improvement of industrial silicon (Si) single crystals produced by the Czochralski (Cz) method has been demanded for high performance in electric devices such as LSI and MOSFET. For an improvement in the quality of a Si crystal, a more precise control of the intrinsic point defects (vacancy (*V*), self-interstitial Si atom (*I*)) and grown-in defects (voids and dislocation clusters) is required. A numerical simulation has become a powerful tool supporting the technology of Si crystal growth by the Cz method and for achieving an improvement in the crystal quality. Over the past few decades, several theoretical and numerical models regarding the behavior of intrinsic point defects in a Si single crystal grown by the Cz method have been studied and applied for optimization of the intrinsic point defect distributions [1,2]. Nowadays, the effects of the incorporated dopant and thermal stress in a growing Si crystal on the behavior of the intrinsic point defects have been investigated using a theoretical approach [3,4]. Moreover, a steady-state distribution of the intrinsic point defects in a growing silicon crystal by the Cz method has been studied through a global heat and mass transfer simulation considering the thermal stress and dopant effects [5]. However, the crystal growth process is strictly unsteady, and operating conditions are changing in time with crystal geometry. Thus, the thermal stress and dopant concentration, which impact the intrinsic point defect distribution in the crystal, depend on the growth history. In more detail, the thermal stress strongly depends on the temporal variation of the crystal/melt interface shape changing during the growth process. Also, a non-uniform distribution of the incorporated dopant concentration can be formed in a growing crystal owing to the segregation effect and changes in the melt flow. Therefore, unsteady modeling is necessary to simulate the behavior of intrinsic point defects considering the effect of the temporal variation of the thermal stress and incorporated dopant concentration in a growing Si crystal. In this paper, we provide unsteady simulation results obtained with a two-dimensional (2D) axisymmetric model of Cz Si growth (large diameters of 400 mm) and discuss the effects of the thermal stress and incorporated dopant concentration on the distributions of the *V* and *I* concentrations in a growing Si crystal.

* Corresponding author.
E-mail address: yuji.mukaiyama@str-soft.co.jp (Y. Mukaiyama).

https://doi.org/10.1016/j.jcrysgro.2019.125433
Received 11 October 2019; Received in revised form 11 December 2019; Accepted 15 December 2019
Available online 16 December 2019

2. Mathematical models

2D axisymmetric unsteady simulations were conducted using the Basic module of the *CGSim* software package [6] for computations of the global heat and mass transfer within an entire Cz furnace, taking into account the turbulent convection in the melt, the thermal stress, the incorporation of a dopant into the growing crystal through segregation, and the dynamics of intrinsic point defects in the crystal. Mathematical models used in the simulation are described in this section.

2.1. Global heat, mass transport, dopant transport, and thermal stress

Governing differential equations for momentum, heat transfer (conduction, convection, and radiation), and mass transfer in the computational domain are solved self-consistently in unsteady simulation [7].

Turbulent mixing of the flow in the melt domain is described based on the Reynolds-averaged Navier-Stokes equation approach. A one-equation model is applied to predict the turbulent effective viscosity in the melt [8]. It is worth to note that the gas convection surrounding a Si crystal is ignored because the gas computational domain is unavailable when considering dynamic crystal pulling in an unsteady-state, which is a limitation of the software. However, it is possible to specify gas cooling effect as an extra boundary condition on the crystal surface. Along the free melt surface, the Marangoni effect is accounted for in the boundary condition for the tangential velocity component.

In an unsteady simulation, the geometry of the crystal/melt interface is corrected on each time step, according to the Stefan problem.

Moreover, the computational domain of a Si crystal is changing dynamically in size in accordance with the calculated pulling rate. The volume of the melt computational domain was changed keeping the mass balance between the crystal and melt domain. The computational grids are modified on each time step using the changed geometries of the crystal and melt domains during an unsteady simulation.

In this study, boron (B) was assumed as the dopant species. The dopant species was treated as a scalar, and the transport equation in the melt domain is as follows:

$$\frac{\partial(\rho\Phi_{melt})}{\partial t} + \nabla\cdot\rho\vec{v}\Phi_{melt} = \nabla\cdot(D_{\Phi_{melt}}\nabla\Phi_{melt}) \quad (1)$$

Here, ρ, $\vec{v}$, Φ_{melt} and $D_{\Phi_{melt}}$ are the density of the melt, the velocity of the melt flow, the mass fraction of the dopant species, and the diffusion coefficient in the melt, respectively. In particular, the incorporation of the dopant into the growing Si crystal through segregation, and the mass balance between the crystal and melt are described by the following equations.

$$\Phi_{crystal} = k\Phi_{melt} \quad (2)$$

$$Q_{melt} = -V_{cr}\rho_{crystal}\Phi_{melt}(1-k) \quad (3)$$

Here, Q_{melt}, $\Phi_{crystal}$, Φ_{melt}, and V_{cr} are the mass flux density of the dopant species from the melt to the crystal, the mass fraction of the dopant in the crystal and melt, and the local crystallization rate on the crystal/melt interface, respectively. The parameter $k$is the segregation coefficient. In this study, a well-known value of k for B ($k = 0.8$) was used.

Eqs. (2) and (3) were applied to the crystal/melt interface as the boundary condition of the dopant incorporation.

The thermal stress in the growing crystal is simulated explicitly based on the calculated temperature distribution. As a boundary condition of the thermal stress of the growing crystal, all constraining conditions at the crystal side surface and the crystal/melt and seed/crystal interfaces are assumed to be free. The respective equations are iteratively solved using a solver based on the finite-volume method. The computational grid for the Cz furnace is shown in Fig. 1. The material properties of Si crystal and melt used in the simulations are described in [7]. The power of the main heater is adjusted using the proportional-integral-differential (PID) algorithm according to the specified target growth rate at a triple point.

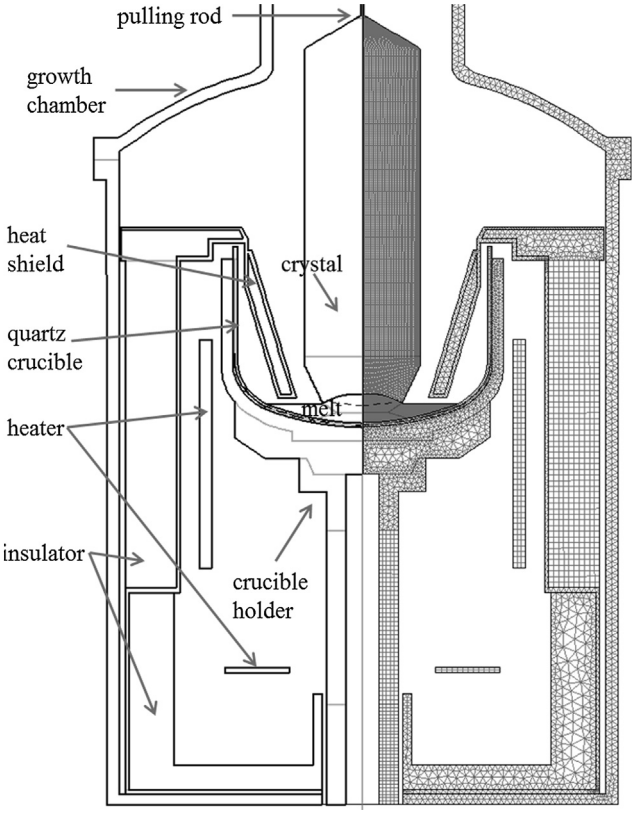

Fig. 1. Material arrangement (left) and computational grids (right) in a Cz furnace.

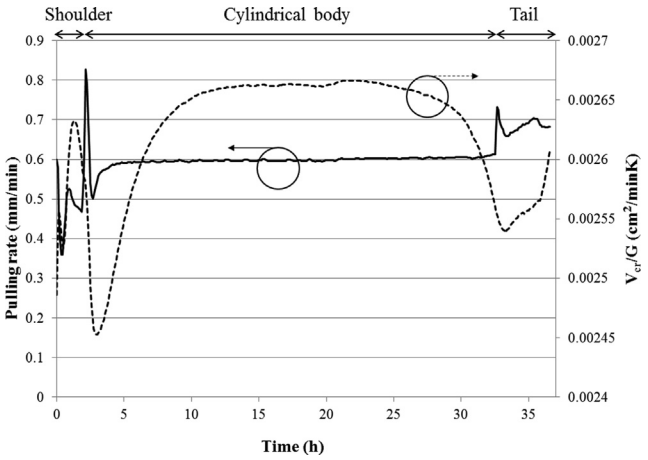

Fig. 2. Temporal variation of pulling rate and Vcr/G.

2.2. Thermal equilibrium concentration of vacancies (V) and self-interstitial Si atoms (I)

The thermal equilibrium concentrations of *V* and *I* are described as a function of the thermal stress and the concentration of the incorporated dopant B in Si crystal [5]. The function was constructed considering the effect of thermal stress and dopant impurities for the formation energy and enthalpy of the point defect. The detailed formula and parameters applied for the function are shown in Ref. [5]. In this function, the isotropic thermal stress is defined as the mean stress, i.e.,

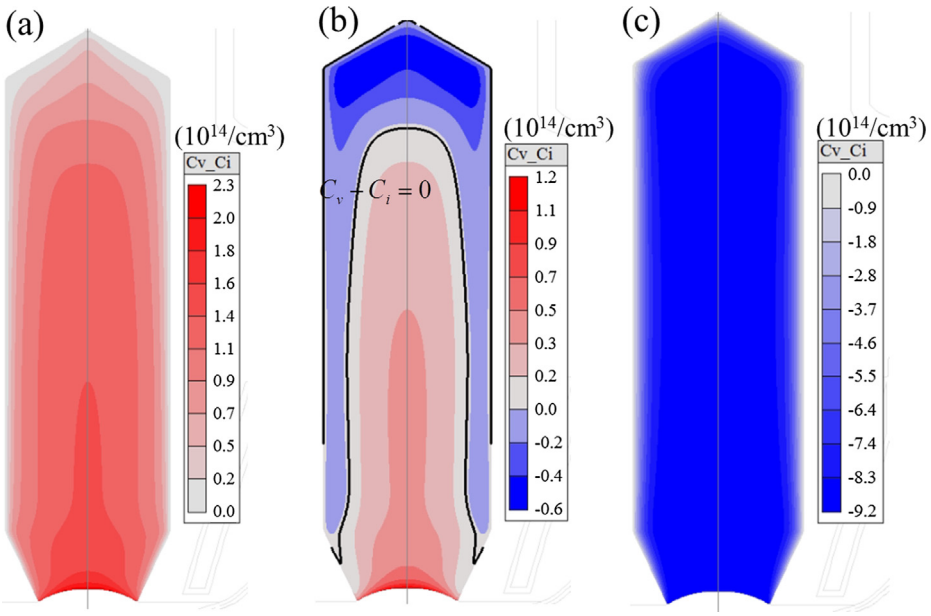

Fig. 3. C_v-C_i distribution in the finally grown Si crystal for (a) undoped state and initial feed concentration of B in the melt at (b) 1.4 (10^{19}/cm^3) and (c) 1.25 (10^{20}/cm^3).

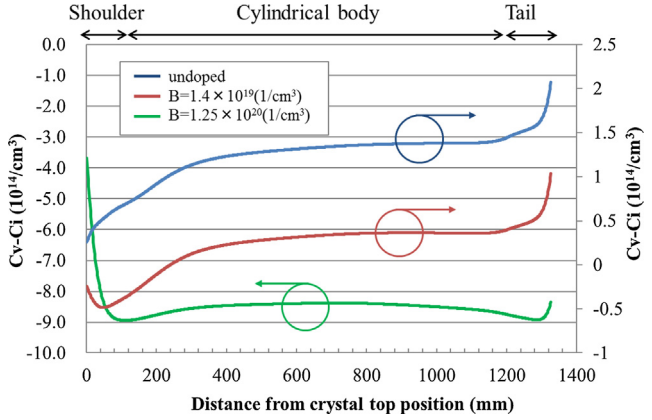

Fig. 4. C_v-C_i distribution along the vertical direction in crystal for undoped (blue line) and initial feed concentration of B in the melt: 1.4 (10^{19}/cm^3) (red line) and 1.25 (10^{20}/cm^3) (green line). (For interpretation of the references to colour in this figure legend, the reader is referred to the web version of this article.)

$\sigma_{mean} = (\sigma_{11} + \sigma_{22} + \sigma_{33})/3$. Predicted thermal stress as a part of global heat transfer modeling is explicitly used for the calculation of the thermal equilibrium concentration of the intrinsic point defects. The thermal stress near the crystallization front is rather approximately planar and not isotropic. Therefore, the concentrations of V and I are the corrected concentrations under a planar stress with the correction parameters [5]. Moreover, the effect of the incorporated dopant B on the formation of the intrinsic point defects is considered as described above. Calculated B concentration in the crystal is used for the calculation of the thermal equilibrium concentration of the point defects.

The functions of the thermal equilibrium concentration are applied for the crystal/melt interface and crystal side surface as the boundary conditions for the point defect transport simulations.

2.3. Point defect dynamics in growing Si crystal

In this investigation, a 2D axisymmetric approximation model was used for V and I dynamics to simulate the distribution of the point defect concentration in a growing Si crystal. This model describes the point defect formation at the crystal/melt interface and the subsequent incorporation into the crystal through advection based on the crystal pulling rate, diffusive transport, and recombination inside the growing bulk crystal. The unsteady-state governing equations for the point defect dynamics in a growing crystal are as follows:

$$V_p \cdot \nabla C_k = \nabla \cdot (D_k \nabla C_k) + 4\pi a_r (D_V + D_I) \times \exp\left(\frac{-\Delta G}{k_B T}\right)(C_{Ie} C_{Ve} - C_I C_V), \quad (4)$$

$$D_k = D_{k,0} \times \exp\left(\frac{-\Delta G_{Dk}}{k_B T}\right), \quad (5)$$

Here, k denotes V or I, and C_k and D_k are the concentration and diffusion coefficients of the point defects, respectively. The pre-exponential factor $D_{k,0}$ and activation energy ΔG_{Dk} were proposed in [9,10]. Furthermore, the local diffusivity in the crystal depends on the local crystal temperature calculated using the global heat and mass transfer simulations. The equilibrium concentrations C_{Ie} and C_{Ve} are the functions of the local temperature, thermal stress, and concentration of dopant B (see Section 2-2). In the advection term of Eq. (4), V_p represents the calculated pulling rate. The last term in Eq. (4) represents the recombination rate, which depends on the local temperature, capture radius a_r, and free energy barrier of the recombination (ΔG) [5].

3. Results and discussion

A schematic view of the Cz furnace, its components and the grid distribution used for the numerical simulations are shown in Fig. 1. The furnace geometry and basic process conditions for the Cz Si growth were borrowed from Ref. [11]. The diameter of the crystal and the height of its finally grown crystal were 400 mm and 1320 mm, respectively.

In addition, the rotation speeds of the crucible and crystal were 8 and 13 rpm with opposite rotation directions, respectively. In this section, the results of the numerical simulation are shown, and the contributions by the transient behavior of the incorporation of B through segregation and the thermal stress on the distribution of the intrinsic point defects in Si crystal growing by the Cz method are discussed.

Fig. 2 illustrates the calculated temporal variation of the crystal

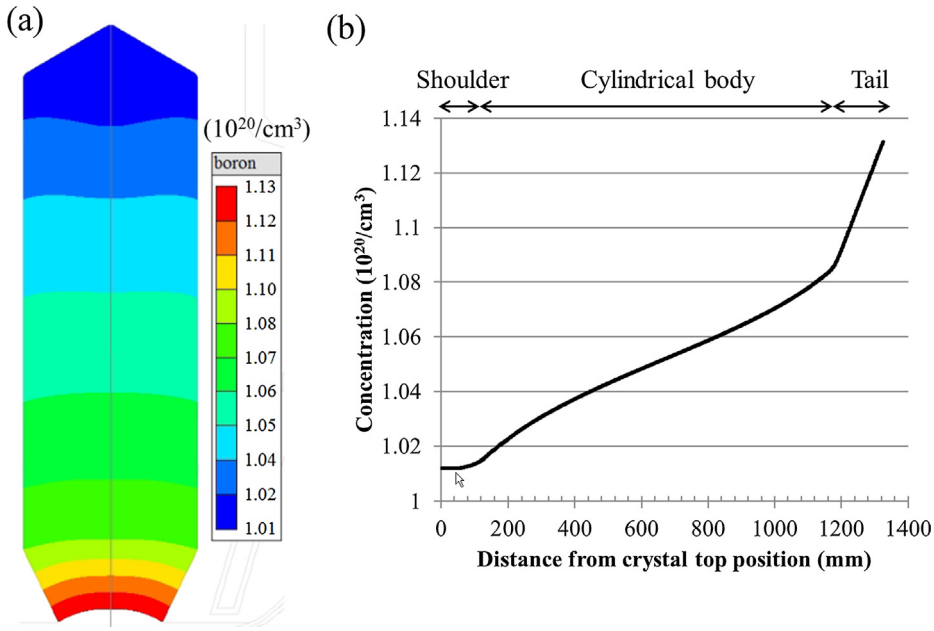

Fig. 5. B concentration distribution (a) in the finally grown Si crystal and (b) along the vertical direction in crystal for the initial feed concentration of B: 1.25 (10^{20}/cm^3).

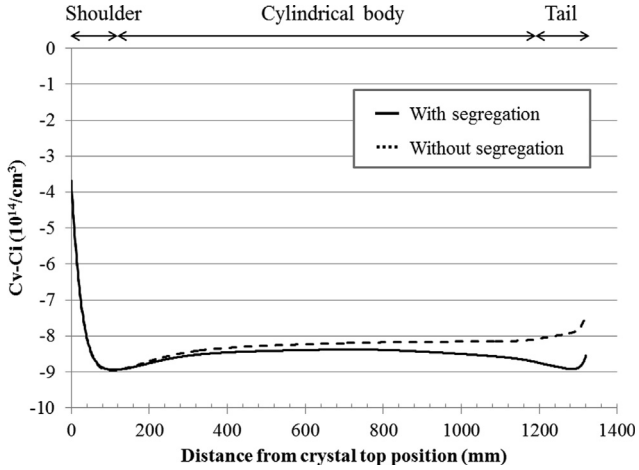

Fig. 6. C_v-C_i distribution along the vertical direction in crystal for cases with and without segregation for the initial feed concentration of B in the melt: 1.25 (10^{20}/cm^3).

pulling rate and Vcr/G during the growth process. Here, Vcr and G are the calculated local crystallization rate and the axial temperature gradient in crystal at the center of crystal/melt interface, respectively. It is well known that the value of Vcr/G is one of the most important parameters to describe the general behavior of intrinsic point defects in a growing crystal. According to Voronkov's theory [1], higher and lower Vcr/G values enhance the incorporation of *V* and *I* into the growing crystal, respectively.

Fig. 3 shows the C_v-C_i value distributions in the finally grown Si crystal for various feed concentrations of B in the melt. It should be noted that the thermal stress effect for the point defects formation were considered for all cases. The value of C_v-C_i represents the difference between the *V* and *I* concentrations, which determines the dominant defect type in the growing crystal. As shown in Fig. 3, with an increase in the concentration of B, C_v-C_i decreases, and the *I*- rich region becomes dominant within the entire crystal area. This dependency on the B concentration was previously discussed [5]. The concentrations of the incorporated *V* and *I* depend on the types and concentrations of dopants. This is because the electrical state and local strain around the dopant atoms change depending on the types and sizes of dopants, which lead to the change in the formation energies of *V* and *I*. In case of B, a higher B concentration decreases the formation energy of *I* and promotes the formation of *I* in the growing Si crystal.

Fig. 4 shows the C_v-C_i distribution in the vertical direction at the center position of the finally grown crystal for various concentrations of B shown in Fig. 3. As described above, C_v-C_i decreases with an increase in the B concentration. Furthermore, C_v-C_i commonly increases in the initial cylindrical body and tail stages for all cases. These behaviors can be explained by the temporal variation in the Vcr/G value shown in Fig. 2 independent of the effect of B concentration. The increase in Vcr/G parameter promotes the incorporation of vacancies *V* into the growing crystal and an increase in C_v-C_i during the initial cylindrical body and tail stages. To investigate the effect of the non-uniform distribution of the incorporated B concentration on the intrinsic point defect distribution in the growing Si crystal, we performed a comparison of the C_v-C_i distributions between two cases, namely, with and without a B segregation effect. For the highest B feed concentration case 1.25 (10^{20}/cm^3), Fig. 5 shows the distribution of the incorporated B concentration in the whole grown crystal and along the symmetry axis of the crystal.

As shown in Fig. 5(a) and (b), the incorporated B concentration increases from the crystal shoulder to the tail. This implies that the incorporation of B increases from the shoulder to the tail stage during the growth process. Fig. 6 shows C_v-C_i in the finally grown crystal for cases with and without B segregation. Without segregation, the initial B concentration was assumed to be constant during the growth process. We can see that C_v-C_i with B segregation is lower than that without segregation effect, particularly during the cylindrical body and tail stage corresponding to the stage when the B incorporation increases. This indicates that the increase in the incorporation of B into the growing crystal enhances the *I*- formation and decreases C_v-C_i during the cylindrical body and tail stage.

To investigate the effect of the thermal stress transient variation during the growth process on the intrinsic point defect distribution in the growing crystal, a comparison of the C_v-C_i distributions both with and without a thermal stress effect was provided. Fig. 7(a) shows the temporal variation of the thermal stress at the center crystal position near the crystal/melt interface during the growth process. Here, the

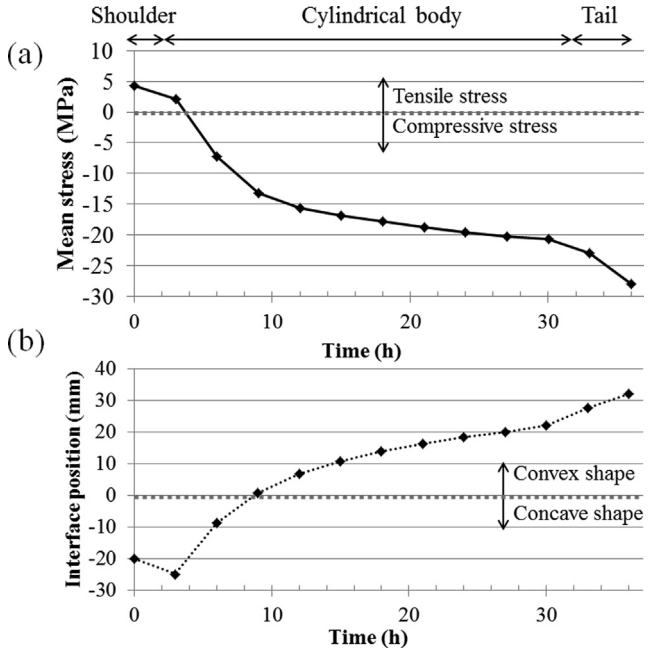

Fig. 7. Temporal variation of (a) the thermal stress near the crystal/melt interface and (b) the interface position.

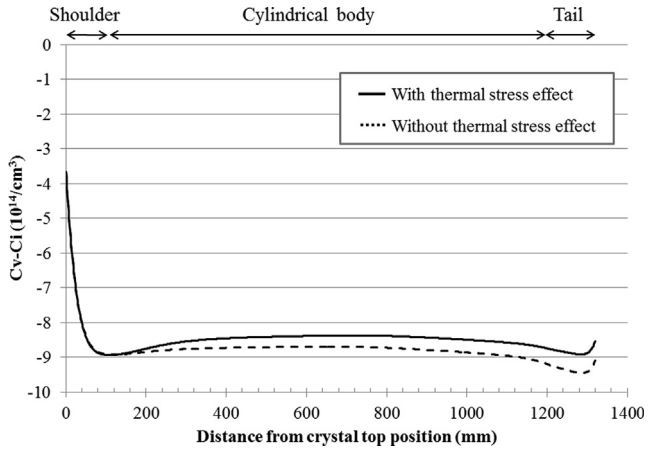

Fig. 8. C_v-C_i distribution along the vertical direction in crystal for cases with and without the thermal stress effect for the initial feed concentration of B in the melt: 1.25 (10^{20}/cm^3).

positive and negative values indicate the tensile and compressive stresses, respectively. As shown in Fig. 7(a), the tensile stress during the shoulder stage changes into a compressive stress during the cylindrical body stage, and the magnitude of the compressive stress increases toward the tail stage. The reason for the change in the thermal stress is related to the variation in the crystal/melt interface geometry during the growth process. Fig. 7(b) illustrates the unsteady variation of the crystal/melt interface deflection from the triple point position. Here, the positive and negative values indicate the convex and concave shapes, respectively. The crystal/melt interface geometry changes from a concave to a convex type between the shoulder and initial cylindrical body stage. Moreover, the convex shape becomes more deflected toward the tail stage. More convex interface shape increases the temperature gradient and further compressive thermal stress near the crystal/melt interface.

Fig. 8 shows C_v-C_i in the finally grown crystal for with and without considering the thermal stress effect. The value of C_v-C_i of the case with a thermal stress effect is higher than the case without a thermal stress effect. In particular, C_v-C_i starts to increase from the upper region of the cylindrical body corresponding to the initial cylindrical body stage when the compressive thermal stress increases. This implies that the increased compressive thermal stress promotes the *V* formation in the growing crystal. This is due to the change in the formation enthalpy of *V* under the compressive thermal stress. According to the previous work [5], it has been found that the thermal stress decreases the formation enthalpy of *V* and promotes the formation of *V*.

In our previous work [5], constant concentration of the incorporated dopant and short crystal length were applied for the prediction of the point defect distribution. However, according to the above results, it is found that the time variation of the dopant distribution and thermal stress significantly affect the point defects distribution during long term Si single crystal growth. Therefore, we think unsteady simulation is required to accurately predict the point defects distribution in the growing crystal. In particular, it should be strong tool to achieve the long Si single crystal with uniform crystal quality.

4. Concluding remarks

A theoretical model for the thermal equilibrium concentration considering the effects of the thermal stress and incorporated dopant was implemented in the crystal growth simulation software *CGSim* package. We conducted an unsteady simulation with a 2D axisymmetric model of the Cz 400 mm diameter Si crystal growth and studied contributing effects of transient incorporation of B through segregation and the thermal stress variation on the distribution of the intrinsic point defects in the growing Si crystal. Our results indicated that the temporal variation of the thermal stress and non-uniform dopant B concentration noticeably impact the intrinsic point defect distribution in the grown Si crystal. This investigation using an unsteady simulation provides essential insight into the behavior of the point defects related to the transient of the thermal stress and dopant incorporation for long term Si single crystal growth by the Cz method.

Declaration of Competing Interest

The authors declared that there is no conflict of interest.

Acknowledgement

This work is partially supported by the JSPS KAKENHI (grant numbers 25390069 and 16K04950) and the Foundation for Assistance to Small Innovative Enterprises (FASIE, Russia) within the ERA.Net RUS Plus Project (grant number 295ГР/21031).

References

[1] V.V. Voronkov, R. Falster, J. Appl. Phys. 86 (1999) 5957.
[2] T. Sinno, Electrochem. Soc. Proc. PV2002-2 (2002) 212–223.
[3] J. Vanhellemont, J. Appl. Phys. 110 (2011) 063519.
[4] K. Sueoka, E. Kamiyama, J. Vanhellemont, J. Crystal Growth 363 (2013) 97.
[5] Koji Sueoka, Yuji Mukaiyama, Susumu Maeda, Masaya Iizuka, Vasif M. Mamedov, ECS J. Solid State Sci. Technol. 8 (4) (2019) P228–P238.
[6] http://www.str-soft.com/products/CGSim/.
[7] V.V. Kalaev, D.P. Lukanin, V.A. Zabelin, Yu.N. Makarov, J. Virbulis, E. Dornberger, W. von Ammon, Mater. Sci. Semicond. Process. 5 (2003) 369–373.
[8] M. Wolfshtein, Int. J. Heat Mass Transf. 12 (1969) 301.
[9] K. Sueoka, E. Kamiyama, J. Vanhellemont, J. Appl. Phys. 114 (2013) 153510.
[10] K. Nakamura, T. Saishoji, J. Tomioka, in: Semiconductor Silicon 2002, PV 2002-2, The Electrochemical Society Proceedings Series, 2002, pp. 554.
[11] Y. Shiraishi, K. Takano, J. Matsubara, T. Iida, N. Takase, N. Machida, M. Kuramoto, H. Yamagishi, J. Crystal Growth 17 (2001) 229.